

FORCED UNBINDING OF THE AVIDIN-BIOTIN COMPLEX

Vincent T. Moy*, Ernst-Ludwig Florin, Matthias Rief, Markus Ludwig & Hermann E. Gaub

Physikdepartment, Technische Universität München, 85748 Garching

**Department of Physiology and Biophysics*

University of Miami School of Medicine, Miami, FL 33101-6430

Abstract. Measurements of unbinding force of individual complex, in combination with thermodynamic analysis, were used to develop a model for the dissociation of the avidin-biotin complex. Atomic force microscope (AFM) measurements of the unbinding force of five avidin-biotin homologues were found to be proportional to the enthalpy change of complex formation, but independent of the free energy change. An examination of the avidin-iminobiotin system revealed that although the equilibrium binding constant varied by 5 orders of magnitude over pH range between 4 and 10, the unbinding force remained constant. These results are consistent with a model where the initial unbinding process is conservative, followed by entropic rearrangement after the avidin-biotin bond had ruptured.

1. Introduction

Specific molecular recognition between ligand and receptor is necessary to provide the selectivity to regulate the elaborate organization in multi-component biological systems. Over the past decade, significant progress has been made to elucidate the nature of these interactions, particularly in the identification, isolation and structural analysis of numerous ligand-receptor complexes that are of principle physiological importance. In addition, various novel biophysical methods (1-3), as well as theoretical treatments (4,5), have contributed to the current advances during this period.

In recent years, focus has been directed towards the force measurement as a means of probing the dynamics and functions of protein-protein interaction. The mechanical stability of ligand-receptor complexes formed by structural proteins such as actin and myosin, and intercellular adhesion molecules play a critical role in their function. In this article, we summarize the application of stochastic unbinding measurements towards the investigation of the dissociation pathway of avidin-biotin complex. Several factors contributed to our selection of this particular system, including the availability of thermodynamic and structural data (6,7).

2. Specific interaction between avidin and biotin

Developments in scanning probe microscopy (i.e., STM, AFM and NSOM) have provided novel techniques to probe the micro-environment of the surfaces with unparalleled spatial resolution and sensitivity (8-11). The atomic force microscope (AFM) is well suited for studying samples in aqueous environment and has evolved into a standard technique in the investigation of biological systems. With chemical modification of the tip, the AFM has been used to measure the interaction between the functional groups on the tip surface and an opposing substrate (12-16). In Fig. 1, we present a protocol for the derivatization of AFM tips with avidin, which we used in the investigation of the interaction between biotin and avidin.

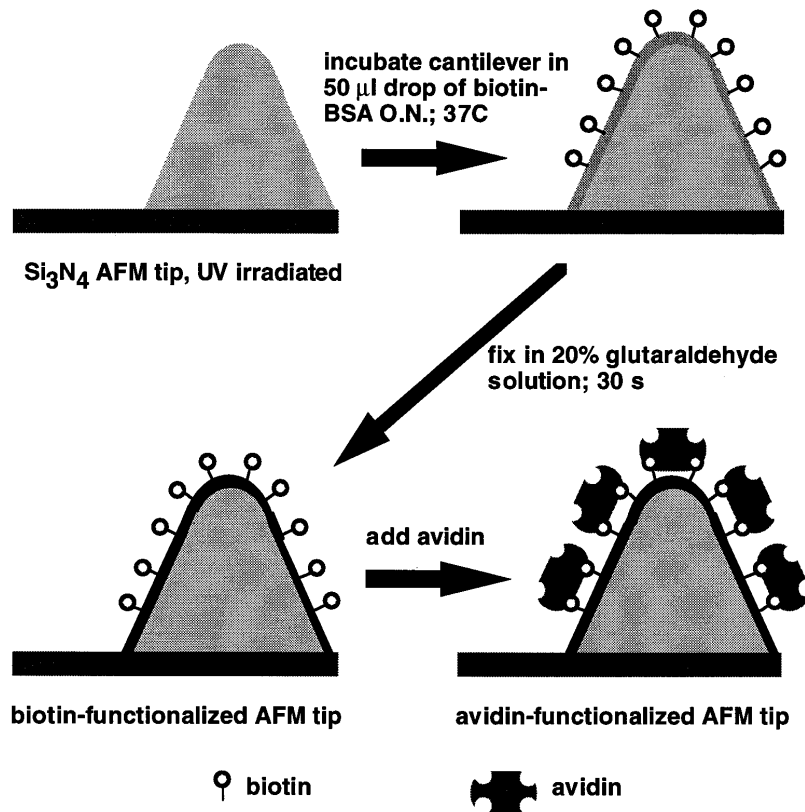


Figure 1. Preparation of avidin-functionalized AFM tips. Si₃N₄ cantilevers from Digital Instruments (Santa Barbara) were irradiated with ultraviolet light for 30 minutes and incubated in 50 μ l solution of biotinamidocaproyl-labeled bovine serum albumin (biotin-BSA, Sigma) in PBS (10 mM P₀⁴⁻², 140 mM NaCl, pH 7.2) at 37° C. Following the adsorption of the biotin-BSA, the cantilevers were rinsed 3 times with PBS and dipped in a fresh 20% solution of glutaraldehyde (Sigma) for about 30 seconds to stabilize the protein film. The modified cantilevers were washed with PBS and stored at 4° C until needed. The biotin-functionalized tips can be prepared several days in advance, however the attachment of the avidin was carried out just prior to an experiment. Avidin was coupled to the tips during the 5 minutes incubation in a 40 μ l drop of avidin (1 mg/ml) at room temperature.

A series of force measurements carried out on a biotinylated agarose bead using avidin functionalized AFM tips is presented in Fig. 2. In these measurements, the interaction between AFM tip and sample is determined from changes in the deflection of the flexible cantilever. The force measurement consists of an approach trace, followed by a retraction trace. Initially, the surfaces are brought together by the piezo element. After contact, further extension of the piezo presses the tip against the sample. During retraction, the tip remains in contact with the sample until the spring constant of the cantilever exceeds the gradient of the interfacial force. In Fig. 2A we measured an adhesive force of 15 nN, corresponding to the interaction of approximately 100 molecular complexes. The measured value of the adhesive force is dependent on the preparation of the AFM tip and the indentation of the tip into the elastic sample. The avidin-functionalized AFM tips were stable, remaining active after several hundred measurements over a fixed area of the sample. Free avidin (Fig. 2B) or free biotin, but not BSA inhibited this adhesive interaction. Furthermore, tips coated with just biotin BSA, but no avidin, did not exhibit any adhesive interaction. Together these findings demonstrate that the adhesive interaction is specific.

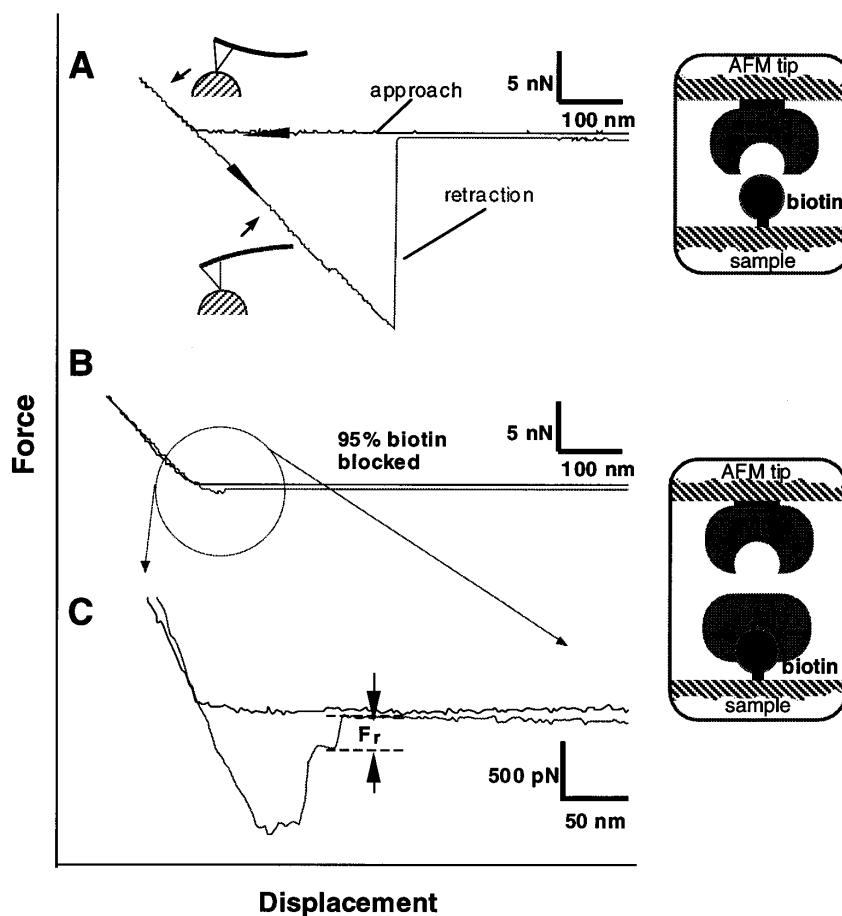


Figure 2. (A) Force measurements between avidin-functionalized AFM tip and biotin-derivatized agarose bead, and (B) after addition of soluble avidin (50 $\mu\text{g/ml}$). (C) Magnification of B. Measurements were carried out with the tip of a scanned stylus AFM aligned directly over the center of the bead. AFM cantilevers were calibrated with a reference spring, previously calibrated with defined weights. The total distance traveled by the piezo during a scan cycle (approach and retraction traces) was 8 μm at a scan rate of 1 Hz. Measurements were made in PBS buffer.

3. Adhesion between individual avidin-biotin pairs

The unbinding of a single avidin-biotin complex was observed when most of the biotin on the agarose bead was blocked with soluble avidin (14). A representative force scan measurement obtained under these conditions is shown in Fig. 2C. A histogram of rupture forces (designated as F_r in Fig. 2) derived from more than 300 force measurements is plotted in Fig. 3 and shows 5 equally spaced maxima starting from the origin. We interpret the value of the first peak, centered at 160 pN, to be the unbinding force of a single avidin-biotin complex and attribute the subsequent maxima in the histogram to integer multiples of this interaction. To demonstrate that this value is characteristic of the avidin-biotin system, measurements from a set of five different avidin-biotin homologues were carried out and summarized in Fig. 4. As shown, the values of the unbinding force varied from 85 ± 10 pN for avidin-*iminobiotin* to 257 ± 15 pN for streptavidin-biotin.

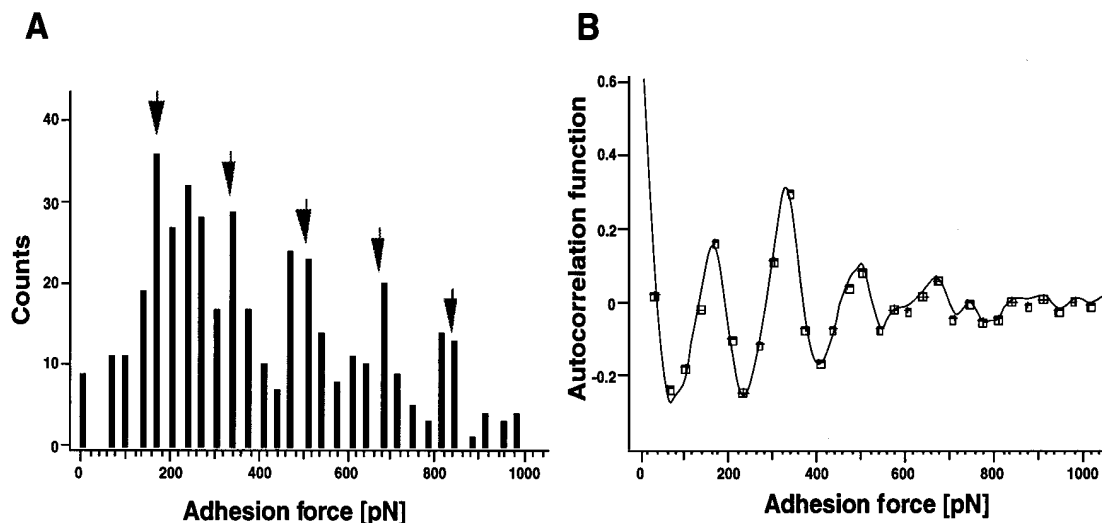


Figure 3. (A) Histogram of rupture forces of avidin-biotin complexes. The rupture force was derived from the deflection of the cantilever immediately prior the contact separation. (B) Autocorrelation analysis of the histogram.

4. Correlation between forces and energies

Insight into the mechanism of the biotin-avidin interaction can be obtained from an analysis of the correlation between the unbinding force of the complex and thermodynamic observables (17). In this analysis, we examined the properties of a series origin. We interpret the value of the first peak, centered at 160 pN, to be the unbinding of avidin-biotin homologues, assuming that the homologues represent minor perturbations of the native avidin-biotin system. From the data tabulated in Fig. 3, a linear relationship between unbinding forces and enthalpy changes is apparent, suggesting that the enthalpy functions in this series of avidin-biotin homologues are invariant during the transition from the bound state to the position of bond rupture. It can also be interpreted that the net change in enthalpy of the binding process stems from formation the bonds occurring at the final docking of the biotin into avidin binding pocket. Accordingly, the work required to unbind the complex reflect the enthalpic energy of the bond formation.

For discussion, it is convenient to divide the intermolecular dissociation potential into two regimes, separated at G^r , the position of bond rupture. In a static model of this process, the rupture point occurs at the steepest point in the free energy potential. Although our force measurements cannot directly provide information on processes that take place beyond bond rupture, we can made inferences from the analysis of the thermodynamic measurements. Fig. 4 reveals no obvious correlation between unbinding force and free energy change. Noting that the free energy values corresponds to changes between the equilibrium bound and dissociated states of the system, the divergence in the free energy functions within the series of homologues may reflect differences in the mechanism of entropic dissipation of energy after bond rupture. As illustrated in fig. 5, our model attributes the principal contribution to changes in the free energy after passage through the transition state to entropic rearrangements in the system. In contrast initial unbinding is viewed as a conservative process with minimal change in entropy.

A

Ligand-Receptor	F_u [pN]	ΔH [kcal/mole]	ΔG [kcal/mole]
avidin-biotin	160 ± 20	-21.5	-20.4
avidin-iminobiotin	85 ± 10	-11.6	-14.3
streptavidin-biotin	257 ± 25	-32.0	-18.3
avidin-desthiobiotin	94 ± 10	-13.5	-16.5
streptavidin-iminobiotin	135 ± 15	NA	-12.2

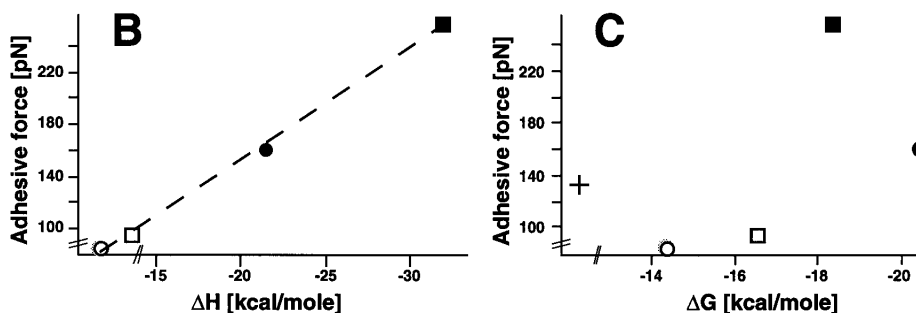


Figure 4. (A) Tabulation of ligand-receptor unbinding forces and the corresponding thermodynamic values of the interacting systems. Thermodynamic values were taken from Green (6), except those for streptavidin, taken from Weber et al. (18). Calorimetric measurements for avidin-desthiobiotin were performed at 25° C in a MicroCal Omega titration calorimeter. Forty 2- μ l injections of ligand solution were titrated at 4 minute intervals into 60 μ M solution of receptor. (B) Plot of unbinding force versus enthalpy. (C) Plot of unbinding force versus free energy. Measurements were carried out in 5 ligand-receptor systems: (i) avidin-biotin (●), (ii) avidin-iminobiotin (○), (iii) streptavidin-biotin (■), (iv) avidin-desthiobiotin (□) and (v) streptavidin-iminobiotin (+).

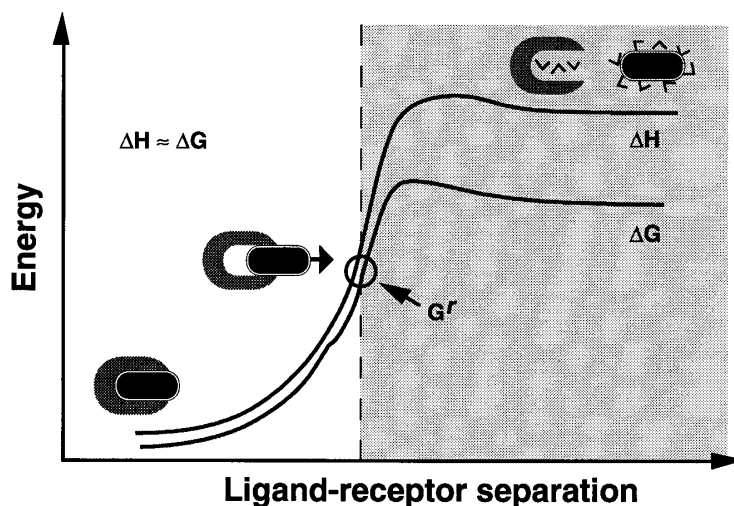


Figure 5. Intermolecular potential of ligand-receptor dissociation. The quantities ΔH and ΔG are the changes in the enthalpy and free energy, respectively, of the process. G^r corresponds to the position of bond rupture. Receptor and ligand are illustrated in gray and black, respectively. The contribution from the solvent is depicted in the dissociated molecules.

Within the framework of our simple model, processes and interactions occurring within the avidin binding pocket should not be dictated by the condition of the solution. To give support to this interpretation, we examined the interaction between avidin and iminobiotin at different pH values. Equilibrium thermodynamic binding studies revealed that the formation of the avidin-iminobiotin complex logarithmically decreases as the pH is lowered below pH 9 (19). This result is consistent with a mechanism in which the free base form of iminobiotin ($pK_a = 11.95$) is required for complex formation. The pH dependence of complex formation is evident in the force measurements between avidin-functionalized tips and iminobiotin beads (Fig. 6A). The observed decrease in adhesion at low pH values may be attributed to a decrease in the number of avidin-iminobiotin complex formed. To determine if there is a noticeable change within the avidin-iminobiotin binding site, the majority of the iminobiotin binding sites on the beads were blocked with free avidin and the unbinding force of the system was measured. The distributions of rupture forces measured at different pH values are plotted in the histograms shown in Fig. 6B. As evident, the unbinding forces are constant within experimental error and independent of the pH of the buffer, indicating that the interactions within the binding site were not affected by the changes in buffer condition.

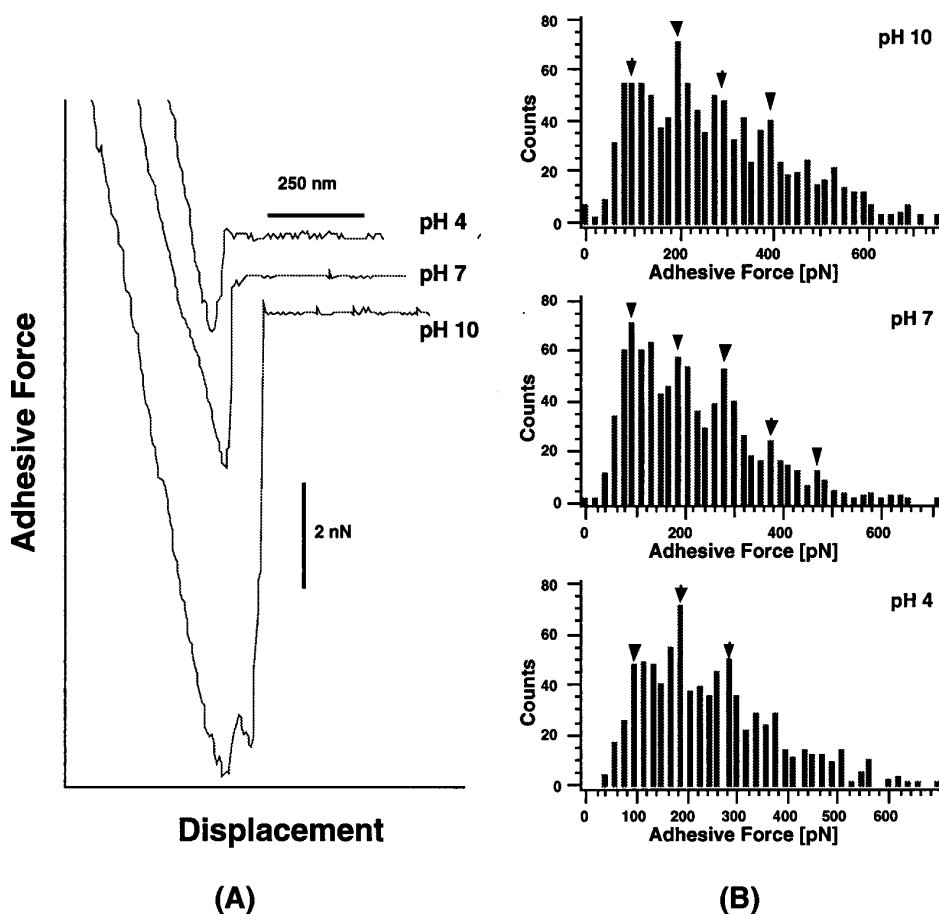


Figure 6. (A) pH dependence of adhesive force between avidin functionalized tip and iminobiotin labeled agarose bead. Shown are the retraction traces of AFM force scan carried out at pH 4, 7 and 10 with adhesive forces of 2, 4, 10 nN, respectively. The buffer used in the pH 7 and 10 measurements was 100 mM sodium phosphate. 100 mM glycine buffer in the pH 4 measurements. (B) Histograms of rupture force between avidin functional AFM tip and iminobiotin-labeled beads. Measurements were carried out at pH 4, 7 and 10.

5. Discussion

The reversible unbinding of the ligand-receptor interaction has been treated theoretically by Bell and others (20-22). For simplicity of analysis we assume that the avidin-biotin interaction takes the form of the Lennard-Jones potential. The total potential of system in a linear external field is given by

$$U_{tot} = 4\xi \left[\left(\frac{\sigma}{r} \right)^{12} - \left(\frac{\sigma}{r} \right)^6 \right] + F_{ex} r$$

Expressed in this form, ξ corresponds to the minimum in the potential at $r = \sqrt[6]{2}\sigma \approx 1.12\sigma$ in the absence of an applied force, F_{ex} . In Fig 7, we illustrate the effects of increasing the external force: (i) a shift in position of the potential minimum to larger displacement and (ii) a lowering of the activation barrier ΔE^* . The total potential of the system is metastable, corresponding to $\Delta E^* = 0$, occurs under the conditions of $U''_{tot} = 0$ and $U'_{tot} \leq 0$. The external force required to reach these conditions is

$$F_u \approx -\frac{2.40\xi}{\sigma} \text{ and is used to define the effective length of the potential as } r_{eff} = \frac{\xi}{F_u} \approx 0.42\sigma.$$

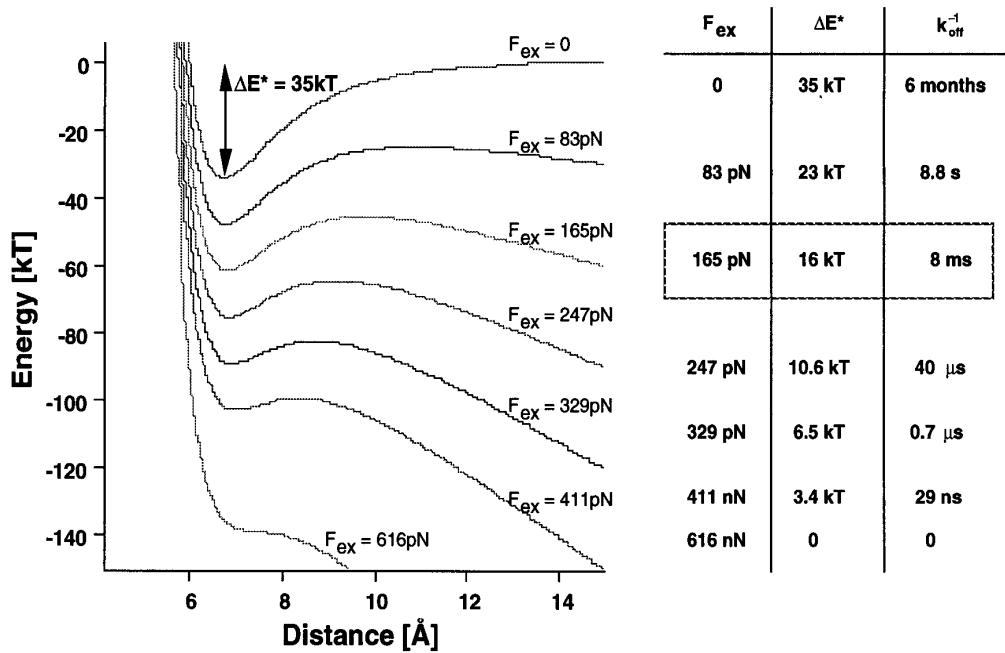


Figure 7. Effects of a linear potential on the dissociation of the binary complex in a Lennard-Jones potential. The values for the parameters ξ and σ are 35kT and 6Å, respectively.

For reversible systems, it is necessary to consider the contribution of thermal excitation in complex dissociation. In Fig 7 we have tabulated the dissociation barrier for selected values of external forces. Assuming that the dissociation kinetic is an exponential function of the ΔE^* , we can calculate the expected survival time of the complex for the different values of F_{ex} . In these calculations, the binding energy and the natural survival time of the avidin-biotin complex were taken from the experimentally measured values of 35kT and 6 months, respectively. Within the framework of this model, the effective length of the L-J potential is uniquely determined for given values of F_{ex} and survival time,

k_{off}^{-1} . An approximation of k_{off}^{-1} is the duration that the avidin-biotin bond is under tension before the complex ruptures. In our experiments, the approximate values for F_{ex} and k_{off}^{-1} are 160 pN and 10 msec, respectively, resulting in a calculated r_{eff} of 2.5 Å. This result gives support to the theory that biotin binding involves more than isolated point interactions. It remains to be determined how the combination of hydrogen bonding and van der Waals interaction can give rise to extended interaction length.

6. Acknowledgements

This work was supported by the Deutsche Forschungsgemeinschaft. Technical assistance from Digital Instruments is gratefully acknowledged.

7. Citations

1. Evans, E., Merkel, R., Ritchie, K., Tha, S. & Zilker, A. in *Studying Cell Adhesion*. (eds. P. Bongrand, P.C., and A. Curtis) in press (Springer, Berlin, 1994).
2. Svoboda, K., Schmidt, C.F., Schnapp, B.J. & Block, S.M. *Nature* **365**, 721 (1993).
3. Wang, N., Bulter, J.P. & Ingber, P.E. *Science* **260**, 1124 (1993).
4. Frauenfelder, H., Sliger, S.G. & Wolynes, P.G. *Science* **254**, 1598 (1991).
5. Miyamoto, S. & Kollman, P.A. *Proteins* **16**, 226 (1993).
6. Green, N.M. *Adv. Prot. Chem* **29**, 85 (1975).
7. Livnah, O., Bayer, E.A., Wilcheck, M. & Sussman, J.L. *PNAS* **90**, 5076 (1993).
8. Binnig, G. & Rohrer, H. *Rev. Mod. Phys.* **59**, 615 (1987).
9. Drake, B., et al. *Science* **243**, 1586 (1989).
10. Radmacher, M., Tillmann, R.W., Fritz, M. & Gaub, H.E. *Science* **257**, 1900 (1992).
11. Betzig, E. & Chichester, R.J. *Science* **262**, 1422 (1993).
12. Lee, G.U., Kidwell, D.A. & Colton, R.J. *Langmuir* **10**, 354 (1994).
13. Moy, V.T., Florin, E.-L. & Gaub, H.E. *Colloids & Surfaces* **93**, 343 (1994).
14. Florin, E.-L., Moy, V.T. & Gaub, H.E. *Science* **264**, 415 (1994).
15. Lee, G.U., Chrisey, L.A. & Colton, R.J. *Science* **266**, 771 (1994).
16. Dammer, U., et al. *Science* **267**, 1173 (1995).
17. Moy, V.T., Florin, E.L. & Gaub, H.G. *Science* **266**, 257 (1994).

18. Weber, P.C., Wendoloski, J.J. Pantoliano, F. & Salemme, R. J. *Am. Chem. Soc.* **114**, 3197 (1992).
19. Green, N.M. *Biochem. J.* **101**, 774 (1966).
20. Bell, G.I. *Science* **200**, 618 (1978).
21. Evans, E., Berk, D. & Leung, A. *Biophys. J.* **59**, 838 (1991).
22. see also Evan, E. & Ritchie, K. in this issue.